Science and Technology for Energy Transition **79**, 37 (2024)
© The Author(s), published by EDP Sciences, 2024
https://doi.org/10.2516/stet/2024031

Available online at:
stet-review.org

REGULAR ARTICLE

OPEN ACCESS

Optimisation of exhaust emissions, vibration, and noise of unmodified diesel engine fuelled with canola biodiesel-diesel blends with natural gas addition by using response surface methodology

Ceyla Özgür[1], Erinç Uludamar[2,*], Hakan Serhad Soyhan[3], and Raja Mazuir Raja Ahsan Shah[4]

[1] Adana Alparslan Türkeş Science and Technology University, Department of Energy Systems Engineering, Adana 01250, Turkey
[2] Adana Alparslan Türkeş Science and Technology University, Department of Mechanical Engineering, Adana 01250, Turkey
[3] Sakarya University, Fire and Combustion Research Center, Serdivan 54187, Turkey
[4] Collage of Engineering Technology, University of Doha for Science and Technology, Doha 24449, Qatar

Received: 13 September 2023 / Accepted: 30 April 2024

Abstract. The paper presents methods to determine the optimum input parameters of CNG addition, biodiesel blend ratio, and engine speed to improve engine responses in terms of exhaust emissions, vibration, and noise of CNG-biodiesel-diesel fuelled engines. Box–Behnken based on response surface methodology was used to predict and optimise input parameters. Variance analysis was applied to determine the significant relationship between the input parameters and engine responses. At optimum input parameters (CNG addition = 9.24 L/min, biodiesel blend ratio = 40%, engine speed = 1524.24 rpm), the optimum engine responses of NO_x, CO, CO_2, O_2, engine vibration acceleration, and noise were 93.77 ppm, 438.05 ppm, 1.47%, 18.59%, 37.17 m/s^2 and 91.34 dB[A], respectively. In terms of coefficient determination of R^2, the values were 99.11%, 99.22%, 99.41%, 99.70%, 98.65%, and 98.60% respectively. The correlation between the optimised result and the engine test result showed an acceptable error limit for NO_x, CO, CO_2, O_2, engine vibration acceleration, and noise as 4.2%, 3.8%, 4.9%, 0.25%, 4.12%, and 0.17%, respectively.

Keywords: Optimisation, Biodiesel, Exhaust emissions, Response surface method, Noise, Vibration.

Nomenclatures

BSFC	Brake specific fuel consumption
BTE	Brake thermal efficiency
CNG	Compressed natural gas
CH_3OH	Methanol
CO	Carbon monoxide
CO_2	Carbon dioxide
HC	Hydrocarbon
L/min	Liter per minute
NaOH	Sodium hydroxide
NO_x	Nitrogen oxides
O_2	Oxygen
ppm	Particle Per Million
rpm	Revolutions per minute
TDC	Top dead centre

* Corresponding author: erinculudamar@gmail.com

1 Introduction

The high demand for conventional fossil-based fuels leads to excessive environmental pollution [1, 2]. Therefore, environmentally friendly fuels need to be brought to the fore. Biodiesel which is derived from vegetable oils is one of the most popular alternative fuels to conventional fossil-based fuels since it is biodegradable, non-toxic, and renewable [3, 4]. Similar properties of biodiesel compared to diesel generally require little or no modification on the diesel engine. However, the differences in terms of carbon atom numbers and the O_2-hydrogen bond of the fuels influence the diesel engine operating characteristics [5, 6].

CNG, which is mainly composed of methane, is another type of fuel that can be used in diesel engines to improve exhaust emissions due to its low-carbon composition. The combination of diesel and CNG lowers the combustion temperature and subsequently reduces NO_x emissions [7]. However, the combination of diesel and CNG has some disadvantages such as low combustion efficiency [8].

This is an Open Access article distributed under the terms of the Creative Commons Attribution License (https://creativecommons.org/licenses/by/4.0), which permits unrestricted use, distribution, and reproduction in any medium, provided the original work is properly cited.

Many studies have focused on the enlightenment of these differences in biodiesel from various sources and different fuel blends. For instance, Tosun and Özcanlı [9] conducted engine performance test comparisons between a blend of soybean biodiesel with hydrogen enrichment and 20% nanoparticle additives and pure biodiesel. Pure biodiesel delivered the worst performance characteristic due to the higher viscosity and lower energy content. However, both fuels improved the CO emissions. On the other hand, Keskin *et al.* [10] used crude tall oil with synthesized manganese-based and nickel-based additives in their experiments. It showed that the engine has better performance due to the biodiesel blend's low sulphur content, aromatic content, low viscosity, higher cetane number, and low cloud point.

Rapid predicting performance, optimizing conditions, and designing structures are accomplished using response surface methodology (RSM) and smart optimization algorithms, which rely on a simulation model enhanced by helical inserts in SMMR [11]. In literature, there are many studies about the optimization process [11–13]. Response surface methodology (RSM) is an effective model for predicting the relationship between desired input and output parameters *via* mathematical and statistical techniques [14, 15]. RSM is a collection of statistical and mathematical techniques which is useful for prediction, modelling, and optimisation [16, 17]. RSM can be used to determine the optimum point of various parameters. The Box–Behnken design (BBD) is among the various designs offered within RSM commonly employed for designing experiments to analyze the performance and emissions of biofuel-powered engines. BBD requires fewer tests, leading to reduced effort, decreased expenses, and a quicker turnaround compared to the complete factorial design. Additionally, when contrasted with the central composite design, BBD proves to be more efficient regarding the ratio of model coefficients to the total number of trials [18].

Shirneshan *et al.* [19] implemented RSM to study the effect of biodiesel from waste cooking oil on the operating parameters of four-cylinder direct injection diesel engines such as engine speed, engine load, and exhaust emissions. From their findings, the optimum conditions with a high desirability of 0.98 were obtained at 77.8% biodiesel percentage in fuel, 41.25% engine load, and 2800 rpm engine speed. Simsek *et al.* [20] used RSM to determine the optimum ratio of liquefied petroleum gas, where the value was 35% at an optimum engine load of 2400 W with less than 4% error ratio.

Singh *et al.* [21] also used RSM for *Spirulina* (L.) microalgae and conventional diesel blends in a single-cylinder variable compression ratio engine. BSFC, BTE, PM, NO_x, and CO_2 were optimised by changing the engine load and the compression ratio. The results showed that maximum BTE, minimal BSFC, and lower emissions could be achieved at an engine load of 63.63%, a compression ratio of 16.5, and a B20 blend (20% biodiesel and 80% diesel). Krishnamoorthy *et al.* [22] used a diesel-waste cooking oil-alcohol blend to study the relationship between fuel, exhaust gas recycling (EGR) rate, injection timing, and variables such as BTE, BSFC, CO, HC, NO_x, and smoke. They concluded that the fuel blend (D50–WCO30–Pe20) injected at a 23° crank angle before TDC with a 15% EGR rate was optimum for exhaust emissions and engine performance at a maximum desirability of 0.974.

Subbaiah *et al.* [23] studied the performance and emission attributes of a Common Rail Direct Diesel Injection (CRDI) engine fueled by a blend of waste plastic oil and biodiesel, incorporating exhaust gas recirculation (EGR). This investigation utilized the Box–Behnken Design (BBD) matrix within the framework of Response Surface Methodology (RSM). They were chosen because the engine's input parameters were IP, load and EGR ratio, and the responses were BSFC, BTE, NO_x and HC. The optimum output engine responses were 21.25% BTE, 0.411 kJ/kW h BSFC, 20.31 ppm HC and 883.29 ppm NO_x, respectively.

Kumar *et al.* [24] implemented artificial neural networks and RSM techniques to predict and optimise palm biodiesel and decanol proportion in the blend for a single-cylinder, four-stroke compression ignition engine. All samples have 10%, 20%, and 30% decanol by volume, and 50% diesel. The study indicated that the optimal proportion was 30% decanol in the fuel blend at a 0.754% desirability rate. Sharma *et al.* [25] performed the Taguchi method and RSM in a diesel engine test with blends of diesel-jojoba biodiesel. Several input parameters were used such as injection pressure, injection timing of fuel, and percentage blends of jojoba-based biodiesel, and engine load as the input parameters. The RSM optimiser showed that the optimum values of corresponding engine responses such as BTE, peak cylinder pressure, exhaust gas temperature, and HC were 34.83%, 5.11 MPa, 444.74 °K, and 38.85 ppm respectively. These engine responses were determined at 25° before TDC injection timing, 21.52 MPa fuel injection pressure, and 24.11% blending of jojoba biodiesel at 80% engine load condition with 0.9024 composite desirability.

From the literature, most works were focused on the optimisation of exhaust emissions of diesel engines, to the best of the authors' knowledge. Therefore, this paper presents the optimisation method on fuel to identify engine vibration and noise (VN) attributes of a diesel engine in addition to exhaust emissions. A Box–Behnken method based on RSM was used to determine the minimum values of exhaust emissions and engine VN of CNG-biodiesel blends by optimising 1) CNG addition, 2) biodiesel blend ratio, and 3) engine speed.

2 Materials and method

In this work, canola oil was used as a feedstock in the transesterification reaction. Canola oil was obtained from local markets. NaOH and CH_3OH were used as a catalyst and an alcohol, respectively.

2.1 Biodiesel production

The production of biodiesel consisted of a 250 ml spherical glass reactor equipped with a condenser, a contact thermometer, and a magnetic stirrer. The production of biodiesel has six processes. 1) 50 ml of oil was placed in the glass

Table 1. Fuel properties of diesel, canola biodiesel, and methane.

Fuel	Density (kg/m^3)	Kinematic viscosity (cSt)	Lower heating value (kJ/kg)	Cetane number	Flash point (°C)
Diesel	837	2.7	45.86	59.3	74.5
Canola biodiesel	883	4.7	38.36	46	120.5
Methane [26, 27]	0.717	–	50.00	–	–
EN 14214	860–900	3.5–5.0	–	Min 51	Min 101

reactor and heated up to 60 °C for each run. 2) 6:1 of CH_3OH to oil molar ratio and 0.5 wt NaOH were used to obtain a sodium methoxide mixture. 3) The solution was added to the preheated canola oil. The transesterification reaction was carried out at 60 °C reaction temperature for 90 min by stirring. 4) After the completion of the transesterification reaction, the crude biodiesel was transferred into a separation funnel and held on for 8 h inside it. 5) The crude glycerine was removed from the methyl ester, and then washed and heated up to 110 °C to eliminate the residuals and water contents. 6) The filtering operation was carried out to separate small impurities inside the methyl ester.

2.2 Preparation of test fuels for engine tests

The obtained biodiesels with transesterification reaction were mixed with a neat diesel at different volumetric ratios (20% and 40%).

The properties of CNG which were used in the engine tests contained 97.37% methane, 2.33% nitrogen, 0.23% ethane, and 0.07% propane. CNG was injected through the intake manifold into intake air with different flow rates; 5 litre per minute (L/min) (CNG5), 10 L/min (CNG10), and 15 L/min (CNG15). The CNG regulator employs a two-stage regulation mechanism. Initially, it lowers the CNG pressure from 200 bar to 12 bar, then further decreases it to 0–1 bar in the second stage. Subsequently, gas flow is managed by a needle vane following the regulator and the flow rate is gauged using a flowmeter positioned after the needle vane.

The fuel properties of diesel and canola biodiesel are given in Table 1.

2.3 Test setup

The engine tests were based on a four-stroke, four-cylinder, direct-injection diesel. The specifications of the engine are given in Table 2 and Figure 1, the schematic of the experimental set-up was illustrated. Engine experiments were performed at 1 atm and between 20–25 °C. The engine was brought to a consistent operating temperature and the fuel line was purged before introducing it with a different fuel. It was then allowed to stabilize before collecting experimental data. The various fuels were tested at engine speeds of 1500 (±3 rpm), 1800 (±3 rpm), and 2100 rpm (±3 rpm) by adjusting the throttle, without any load in order to eliminate the noise and vibration generated by the dynamometer. Moreover, the periphery of the dynamometer was covered with a wooden box which has sound absorber panels inside it. After the engine stabilized, experimental data was collected for 10 s and an average of them was used.

Table 2. Engine technical specifications.

Brand	Mitsubishi canter
Model	4D34-2A
Configuration	In line 4
Firing order	1–3–4–2
Type	Direct injection diesel with glow plug
Displacement	3907 cc
Bore	104 mm
Stroke	115 mm
Power	89 kW@3200rpm
Torque	295 Nm@1800rpm
Weight	325 kg

MRU Delta 1600-V exhaust gas analyser was used to measure exhaust emissions values. Exhaust emissions were analysed *via* MRU Delta 1600-V gas analyser which is able to measure CO, carbon dioxide (CO_2), oxygen (O_2), nitric oxide (NO), and nitrogen dioxide (NO_2) emissions. The range and accuracy of them are; 0–4000 ppm and ±20 ppm; 0%–20% and ±0.5%; 0%–22% and 0.01%; 0–1000 ppm and ±5 ppm; and 0–200 ppm and ±5 ppm, respectively. The device calculates NO_x emissions according to the sum of NO and NO_2 emissions.

Acoustic and vibration data were recorded *via* SoundbookTM universal portable measuring system with SAMURAI v2.6 software from SINUS Messtechnik GmbH. ToughbookTM CF-19 from a Panasonic portable PC was used to record the VN data of the engine. VN data was filtered according to ISO 10816, ISO 7919, and ISO 2954 standards. The vibration measurement range was from 2 Hz to 20 kHz. The sound level meter (SLM) of the software meets the Class 1 SLM according to IEC 60651, IEC 60804, and DIN EN 61672-1:2003 standards. The vibration of the engine was measured in three orthogonal axes (longitudinal, vertical, and lateral). The total engine vibration acceleration (a_{total}) was calculated *via* these values using equation (1).

$$a_{total} = \sqrt{a_{longitudinal}^2 + a_{vertical}^2 + a_{lateral}^2}. \quad (1)$$

Triaxial ICP® accelerometer sensor from PCB electronics model 356A33 and GRAS 46AF 1/2″ LEMO half-inch Free-field Standard Microphone Set were used in the engine test setup. The accelerometer was adhered to the engine

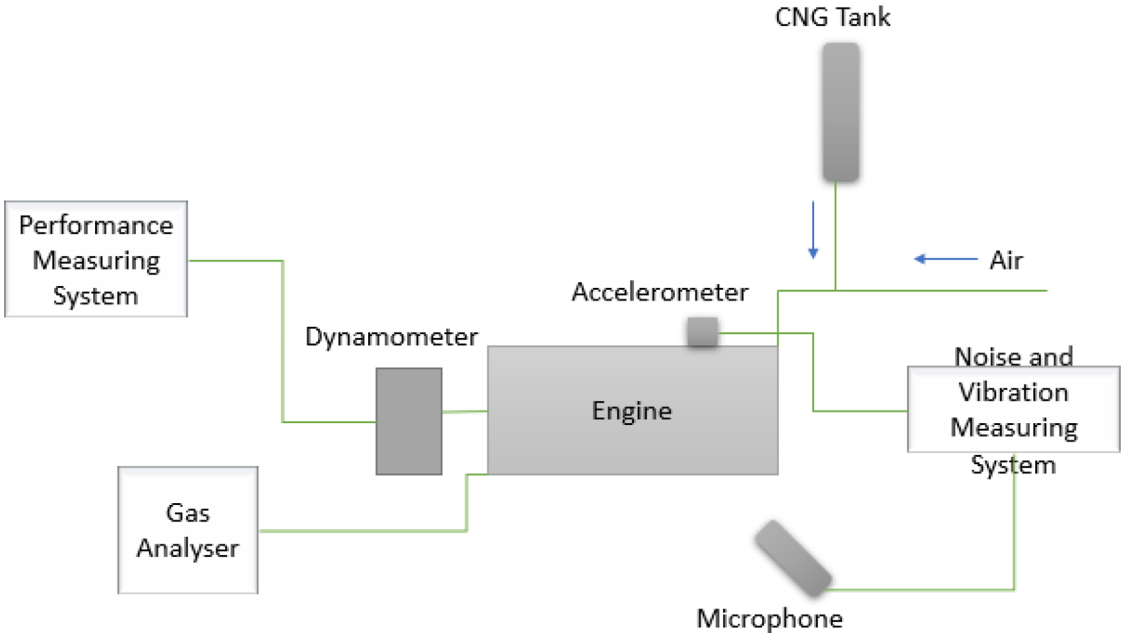

Fig. 1. Schematic view of engine test setup.

Table 3. Input factors and their levels.

Factors	Symbol	Levels		
		−1	0	1
CNG addition (L/min)	X_1	5	10	15
Biodiesel ratio (%)	X_2	0	20	40
Engine speed (rpm)	X_3	1500	1800	2100

support with quick bonding gels to measure the data with high accuracy. The microphone was placed one meter away from the engine.

2.4 Uncertainty analysis

In this work, the experimental combined uncertainty was computed by equation (2). According to the study of How *et al.* [28] and the combined uncertainty was found as 4.80%.

$$\begin{aligned} U_{\text{combined}} = {} & \text{Square root of } \{(\text{uncertainty of CO})^2 \\ & + (\text{uncertainty of CO}^2)^2 \\ & + (\text{uncertainty of NO}_x)^2 \\ & + (\text{uncertainty of vibration})^2 \\ & + (\text{uncertainty of noise})^2\}. \end{aligned} \tag{2}$$

2.5 Modelling and optimisation

RSM involves employing a blend of mathematical and statistical techniques to model and analyze situations where a desired outcome is influenced by multiple variables, to optimize this outcome. Design of Experiment (DOE) serves as a commonly employed tool for attaining the most favourable optimization outcome through an optimal number of experiments. In the optimization process, several DOE techniques are utilized, including fractional design, Full Factorial Design (FFD), the Taguchi method, Box Behnken Design (BBD), and Central Composite Design (CCD) [29]. In this study, Box–Behnken of RSM was used to design and analyse the independent variables and their responses. A BBD is a type of experimental design for response surfaces that does not incorporate a built-in factorial or fractional factorial design. BBDs are employed to generate higher-order response surfaces with fewer required runs compared to a typical factorial approach. The critical parameters are assessed through a BBD experiment. This experimental setup enables achieving a satisfactory fit using a quadratic model with the gathered data points [30].

Three input parameters were used in the design of the experiment using Box–Behnken, namely CNG addition (X_1), biodiesel ratio (X_2), and engine speed (X_3). All input parameters were arranged at three levels (−1, 0, +1) with equally spaced intervals. MINITAB statistical software was used to enhance the RSM model. Table 3 depicts the input parameters and their levels.

A total of 17 engine tests were performed, where these numbers were determined by equation (3) [26].

$$N = 2k(k-1) + C_p \tag{3}$$

where N is the number of engine tests required, k is the number of input parameters and C_p is the number of central points. Statistical 3-D plots, analysis of variance (ANOVA), and coefficient of determination (R^2) were used to interpret the results. For the factors, the polynomial equation (Eq. (4)) is obtained from [27].

$$\begin{aligned} Y = {} & \beta_0 + \beta_1 X_1 + \beta_2 X_2 + \beta_3 X_3 + \beta_{12} X_1 X_2 \\ & + \beta_{13} X_1 X_3 + \beta_{23} X_2 X_3 + \beta_{11} X_{11} + \beta_{22} X_{22} \\ & + \beta_{33} X_{33}, \end{aligned} \tag{4}$$

where Y is the predicted response, β_0 is model constant, X_1, X_2, and X_3 are input parameters; β_1, β_2, and β_3 are linear coefficients; β_{12}, β_{13}, and β_{23} are cross-product coefficients; and β_{11}, β_{22}, and β_{33} are the quadratic coefficients.

The process flow diagram of the applied RSM model is shown in Figure 2. The corresponding NO_x, CO, CO_2, O_2 emissions, and engine VN values as the responses in the engine tests are given in Tables 4 and 5.

Table 6 provides the determined values of R-squared, adjusted (Adj.) R-squared, and prediction (Pred.) R squared.

2.6 Desirability approach of RSM

RSM-based desirability approach was used to optimise process parameters for measuring engine responses. MINITAB statistical software was used for optimisation analysis. Each response was transformed to a dimensionless desirability value (d). It ranges between $d = 0$, which suggests that the response was completely unacceptable, and $d = 1$, which suggests that the response was more desirable. The criteria of this work are to minimise the values of exhaust emissions and engine VN.

3 Results and discussions

3.1 ANOVA method

The significance of the relationship between the input parameters and engine responses was determined by using the ANOVA method. Tables 7 and 8 show the F values and P values of input parameters and engine responses. A "P value" less than 0.05 is considered significant.

3.2 Impacts of input parameters on NO_x emissions

Combustion temperature, combustion duration, and local O_2 concentration are the primary factors of NO_x formation [31]. Figure 3 shows the effects of input parameters on NO_x emissions. As can be seen, the NO_x emissions were decreased with the addition of CNG. The reduction in NO_x emissions was due to the cooling effect of the injection of cold CNG into the combustion chamber. This phenomenon reduced the peak combustion temperature and subsequently reduced NO_x emissions [32].

The ANOVA method showed that NO_x emissions were significantly influenced by CNG flow rate, biodiesel blend ratio, and engine speed. The coefficient of determination of R^2 was 0.9911 and the difference between the adjusted R^2 and predicted R^2 was 0.122 and within the range of 0.2. The obtained quadratic equation for NO_x emissions is given by equation (5).

$$\begin{aligned} NO_x = {} & -162.1 - 3.05X_1 - 0.125X_2 + 0.2317X_3 \\ & - 0.0950{X_1}^2 - 0.00219{X_2}^2 - 0.000043{X_3}^2 \\ & + 0.0225X_1X_2 + 0.00117X_1X_3 \\ & + 0.000375X_2X_3. \end{aligned} \tag{5}$$

3.3 Impacts of input parameters on CO emissions

Figure 4 shows the effects of input parameters on CO exhaust emissions. The formation of CO emissions was due to inadequate O_2 and insufficient combustion quality [33]. CO emissions value decreased with the increase in biodiesel ratio. This phenomenon was due to the fuel-bound O_2 in biodiesel reducing the local fuel-rich zone inside the combustion chamber, therefore enhancing the complete oxidation of fresh carbon atoms or partially oxidised CO to CO_2, and reducing CO emissions. On the other hand, CO emissions increased with the increment in the CNG addition since incoming air was replaced with CNG gas. The ANOVA model provided that the P values of CNG addition flow and engine speed were smaller than 0.0001. The goodness of fit for the CO model was 0.99. The regression formed of CO emissions is given by equation (6).

$$\begin{aligned} CO = {} & -3281 + 15.3X_1 + 1.77X_2 + 3.712X_3 \\ & - 0.585{X_1}^2 + 0.0378{X_2}^2 - 0.000926{X_3}^2 \\ & + 0.1600X_1X_2 + 0.00900X_1X_3 \\ & - 0.00321X_2X_3. \end{aligned} \tag{6}$$

3.4 Impacts of input parameters on CO_2 emissions

CO_2 is the main source of global warming and ozone layer depletion. However, this molecule can be absorbed by plants and algae. Figure 5 gives the effects of input parameters on CO_2 emissions. During the combustion of fuel, due to the insufficient amount of O_2, all carbon molecules did not convert to CO_2 molecules [34]. CO_2 emissions values were increased by using biodiesel compared to conventional diesel fuel as explained in the section impacts of input parameters on CO emissions. The formation of CO_2 is shown in equation (7).

$$\begin{aligned} CO_2 = {} & -9.914 + 0.0358X_1 + 0.00126X_2 \\ & + 0.011572X_3 - 0.001380{X_1}^2 - 0.000024{X_2}^2 \\ & - 0.000003{X_3}^2 + 0.000050X_1X_2 \\ & - 0.000005X_1X_3 + 0.000001X_2X_3. \end{aligned} \tag{7}$$

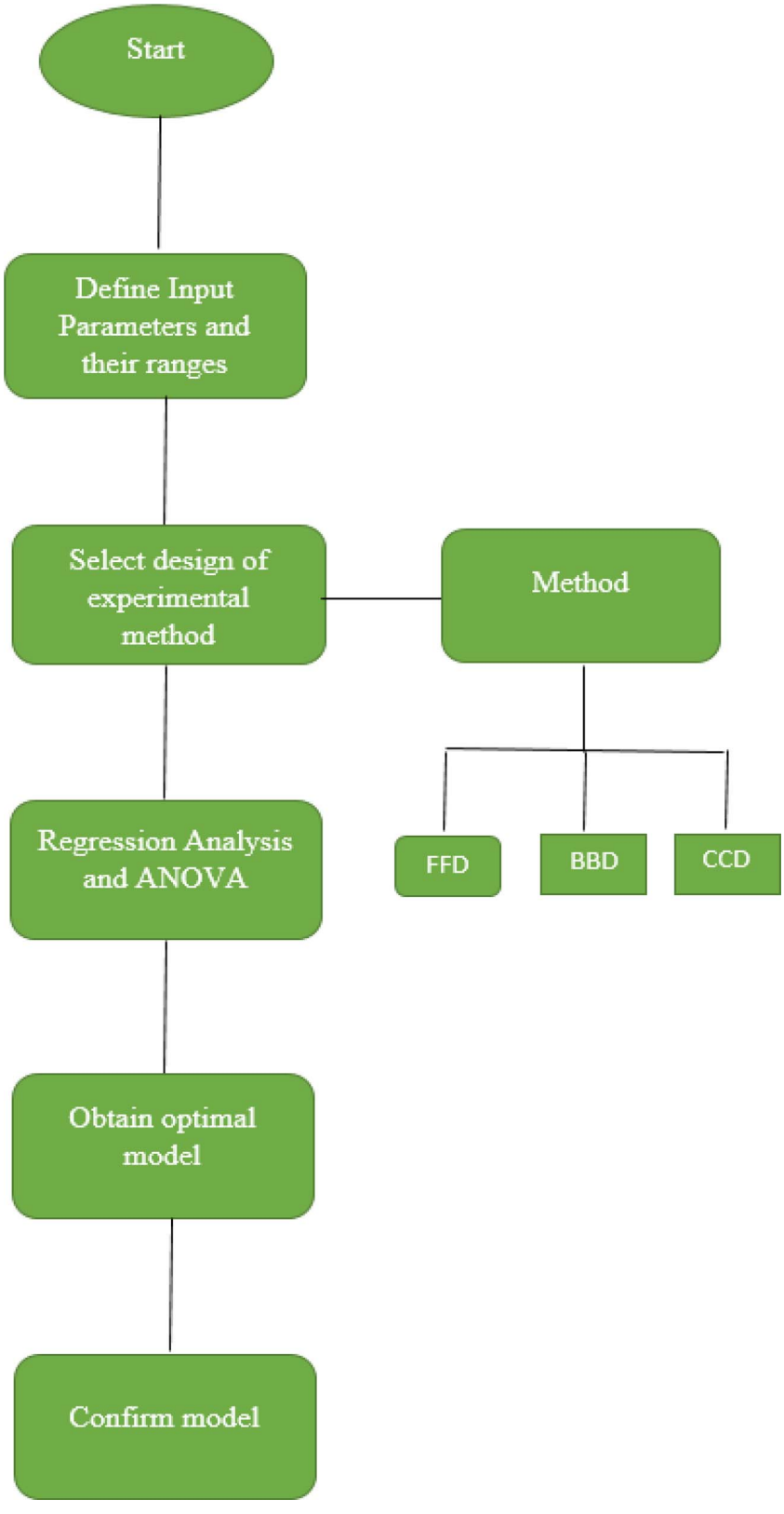

Fig. 2. Flowchart of RSM.

Table 4. Test and predict values of engine responses for NO_x, CO, CO_2, and O_2 emissions for canola biodiesel.

Run	CNG addition (L/min)	Biodiesel ratio (%)	Engine speed (rpm)	Test				Prediction			
				NO_x (ppm)	CO (ppm)	CO_2 (%)	O_2 (%)	NO_x(ppm)	CO (%)	CO_2 (%)	O_2 (%)
1	15	20	2100	121	765	2.18	17.34	123.25	774.63	2.19	17.40
2	10	20	1800	111	623	1.99	17.78	111.00	623.00	2.04	17.78
3	10	20	1800	111	623	1.99	17.78	111.00	623.00	2.04	17.78
4	10	40	1500	85	415	1.38	18.67	89.00	435.25	1.40	18.72
5	15	20	1500	66	508	1.34	19.04	62.25	505.88	1.33	19.00
6	15	40	1800	112	755	2.07	17.43	111.75	736.88	2.07	17.42
7	5	20	1500	92	312	1.32	19.15	89.75	302.38	1.31	19.09
8	15	0	1800	78	730	1.93	17.65	120.88	740.63	1.94	17.64
9	10	0	1500	64	441	1.28	18.80	66.00	432.50	1.29	18.85
10	10	40	2100	153	630	2.30	17.08	151.00	638.50	2.29	17.03
11	10	20	1800	111	623	1.99	17.78	111.00	623.00	2.04	17.78
12	5	40	1800	133	485	2.06	17.52	131.25	474.38	2.06	17.53
13	5	20	2100	140	515	2.19	17.43	143.75	517.13	2.21	17.47
14	5	0	1800	108	524	1.94	17.69	108.25	542.13	1.94	17.70
15	10	0	2100	123	733	2.17	17.35	119.00	712.75	2.15	17.30
16	10	20	1800	111	623	1.99	17.78	111.00	623.00	2.04	17.78
17	10	20	1800	111	623	1.99	17.78	111.00	623.00	2.04	17.78

Table 5. Test and predicted values of responses for VN for canola biodiesel.

Run	CNG addition (L/min)	Biodiesel ratio (%)	Engine speed (rpm)	Test		Prediction	
				Vibration (m/s^2)	Noise dB[A]	Vibration (m/s^2)	Noise dB[A]
1	15	20	2100	52.9	97.1	53.68	96.9000
2	10	20	1800	46.6	91.8	46.60	91.80
3	10	20	1800	46.6	91.8	46.60	91.80
4	10	40	1500	34.6	91.2	36.15	91.36
5	15	20	1500	34.8	91.5	34.33	91.63
6	15	40	1800	46.1	93.2	45.03	92.91
7	5	20	1500	37.9	91.9	37.13	92.10
8	15	0	1800	43.8	92.8	44.58	93.16
9	10	0	1500	39.4	92.3	39.10	91.81
10	10	40	2100	57.4	96.2	57.70	96.69
11	10	20	1800	46.6	91.8	46.60	91.80
12	5	40	1800	47.4	93.6	46.63	93.24
13	5	20	2100	55.1	97.4	55.58	97.28
14	5	0	1800	46.6	93.4	47.68	93.69
15	10	0	2100	56.9	97.1	55.35	96.94
16	10	20	1800	46.6	91.8	46.60	91.80
17	10	20	1800	46.6	91.8	46.60	91.80

Table 6. Model evaluation for canola biodiesel.

Model	R^2	Adj. R^2	Pred. R^2
NO_x	99.11%	97.97%	85.79%
CO	99.22%	98.22%	87.54%
CO_2	99.41%	98.64%	98.01%
O_2	99.70%	99.32%	95.27%
Vibration	98.65%	96.91%	78.40%
Noise	98.60%	96.80%	77.61%

Table 7. ANOVA method for exhaust emissions.

Source	NO_x (ppm)			CO (ppm)			CO_2 (%)			O_2 (%)		
	Sum of squares	*F*-value	*P*-value	Sun of squares	*F*-value	*P*-value	Sun of squares	*F*-value	*P*-value	Sum of squares	*F*-value	*P*-value
Model	9427.38	86.77	0.000	260130	99.09	0.000	1.85913	130.33	0.000	6.29595	262.21	0.000
Linear	9277.00	256.17	0.000	225703	257.94	0.000	1.57883	332.03	0.000	5.30808	663.21	0.000
A-CNG blend	1152.00	95.43	0.000	106261	364.31	0.000	0.00001	0.01	0.932	0.01361	5.10	0.058
B-biodiesel ratio (%)	1512.50	125.30	0.000	2556	8.76	0.021	0.03001	18.94	0.003	0.07801	29.24	0.001
C-engine speed (rpm)	6612.50	547.78	0.000	116886	400.74	0.000	1.54880	977.16	0.000	5.21645	1955.30	0.000
Square	97.63	2.70	0.126	31192	35.65	0.000	0.27975	58.83	0.000	0.98225	122.73	0.000
A^2	23.75	1.97	0.203	901	3.09	0.122	0.00501	3.16	0.119	0.00348	1.30	0.291
B^2	3.22	0.27	0.621	963	3.30	0.112	0.00038	0.24	0.639	0.23501	88.09	0.000
C^2	63.22	5.24	0.056	29269	100.35	0.000	0.26739	168.70	0.000	0.78306	293.52	0.000
2-way interaction	52.75	1.46	0.306	1078	3.70	0.070	0.00055	0.12	0.948	0.00563	0.70	0.580
AB	20.25	1.68	0.236	1024	3.51	0.103	0.00010	0.06	0.809	0.00062	0.23	0.643
AC	12.25	1.01	0.347	729	2.50	0.158	0.00022	0.14	0.718	0.00010	0.04	0.852
BC	20.25	1.68	0.236	1482	5.08	0.059	0.00023	0.14	0.718	0.00490	1.84	0.217
Error	84.50			2042			0.01109			0.01867		
Total	9511.88			262172			1.87022			6.31462		

Table 8. ANOVA method for engine VN.

Source	Vibration (m/s^2)			Noise (dB[A])		
	Sum of squares	*F*-value	*P*-value	Sum of squares	*F*-value	*P*-value
Model	741.685	56.83	0.000	75.2313	54.81	0.000
Linear	725.645	166.81	0.000	55.2075	120.67	0.000
A-CNG blend	11.045	7.62	0.025	0.3613	2.37	0.168
B-biodiesel ratio (%)	0.180	0.12	0.735	0.2450	1.61	0.246
C-engine speed (rpm)	714.420	492.70	0.000	54.6012	358.04	0.000
Square	8.253	1.90	0.218	20.0013	43.72	0.000
A^2	6.711	4.63	0.068	3.1322	20.54	0.003
B^2	1.711	1.18	0.313	1.4533	9.53	0.018
C^2	0.111	0.08	0.790	13.8322	90.70	0.000
2-way interaction	7.788	1.79	0.237	0.0225	0.05	0.984
AB	0.563	0.39	0.553	0.0100	0.07	0.805
AC	0.203	0.14	0.720	0.0025	0.02	0.902
BC	7.023	4.84	0.064	0.0100	0.07	0.805
Error	10.150			1.0675		
Total	751.835			76.2988		

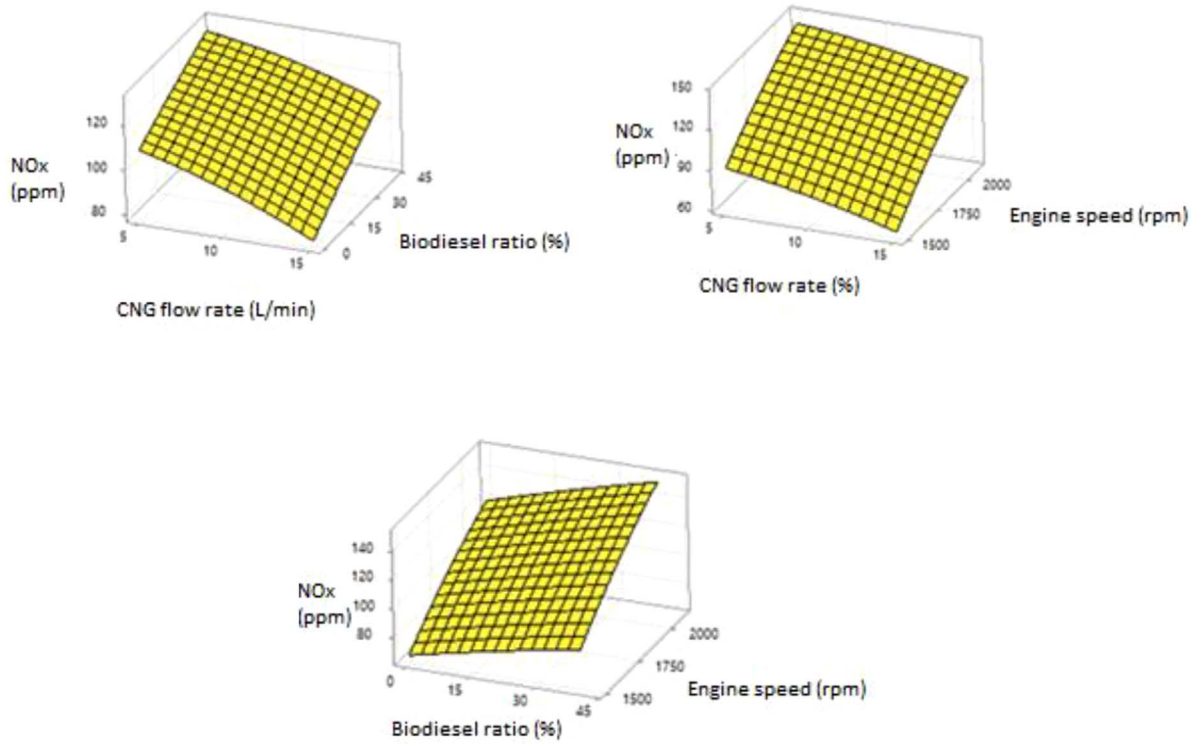

Fig. 3. Impacts of input parameters on NO_x emissions.

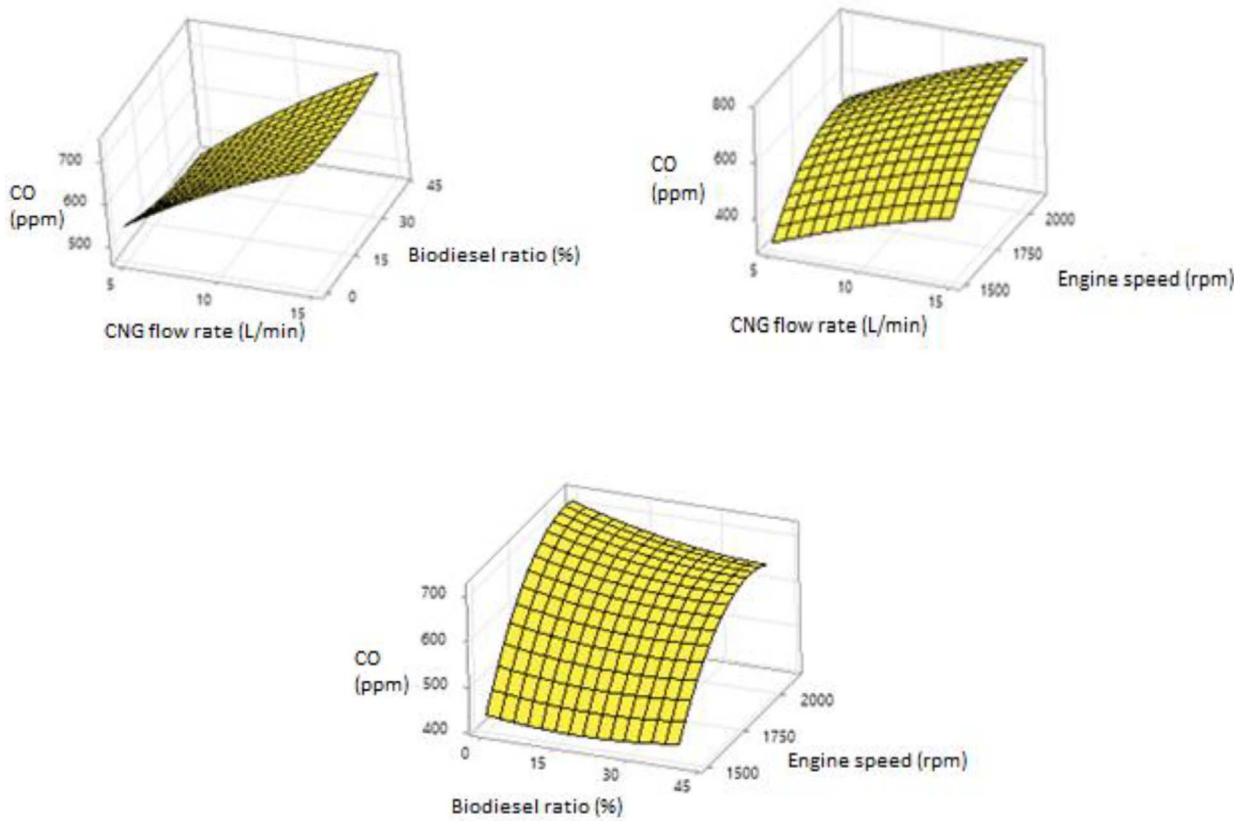

Fig. 4. Impacts of input parameters on CO exhaust emissions.

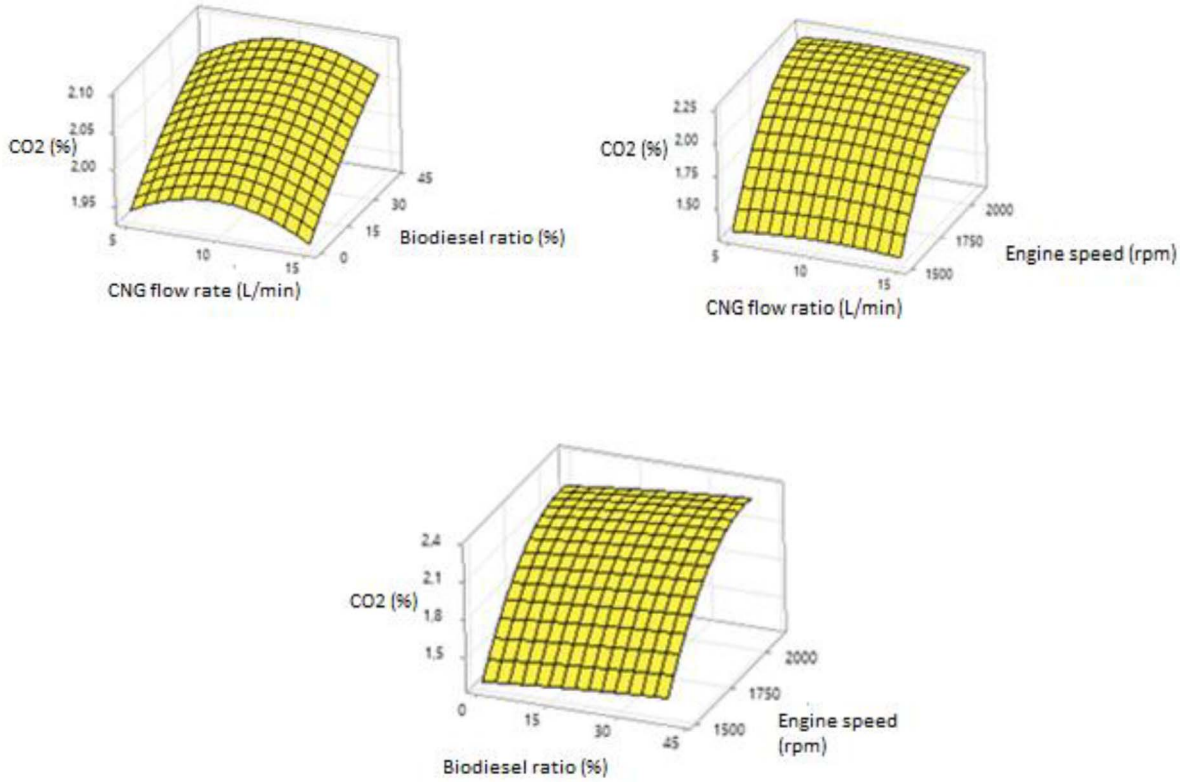

Fig. 5. Impacts of input parameters on CO_2 emissions.

3.5 Impacts of input parameters on O_2 emissions

Extra O_2 molecules may come from some alternative fuels, such as biodiesel. The amount of O_2 in the exhaust gas is one of the important feedback parameters in adjusting the fuel injection duration [35]. In a diesel engine, the occurrence of O_2 molecules in exhaust gases is generally related to an inefficient combustion process since the engine operates at lean air–fuel mixtures. Figure 6 demonstrates the various surface plots of O_2 for different CNG additions, biodiesel ratios, and engine speeds. The formation of O_2 is shown in equation (8).

$$\begin{aligned} O_2 = {} & 38.035 - 0.0347X_1 + 0.03044X_2 - 0.01986X_3 \\ & + 0.00115{X_1}^2 - 0.000591{X_2}^2 + 0.000005{X_3}^2 \\ & - 0.000125X_1X_2 + 0.000003X_1X_3 \\ & - 0.000006X_2X_3. \end{aligned} \tag{8}$$

3.6 Impacts of input parameters on engine vibration

The engine vibration is influenced by the combustion quality, piston movement, fluid impact, and inertia of moving parts [36]. The results in Figure 7 enlighten that the engine vibration decreased with the increment of CNG addition and biodiesel blend ratio. The extra O_2 content of biodiesel and the different combustion properties of CNG can affect the peak pressure rise rate, combustion duration, and ignition delay which results in less engine vibration severity [35, 37]. The engine vibration severity is shown in equation (9).

$$\begin{aligned} a_{total} = {} & -6.5 + 0.43X_1 - 0.506X_2 + 0.0321X_3 \\ & - 0.0505{X_1}^2 + 0.00159{X_2}^2 - 0.000002{X_3}^2 \\ & + 0.00375X_1X_2 + 0.000150X_1X_3 \\ & + 0.000221X_2X_3. \end{aligned} \tag{9}$$

3.7 Impacts of input parameters on engine noise

Combustion, mechanical, intake, and exhaust noises are the main sources of diesel engine noise [38]. Figure 8 shows the decrease in engine noise due to the engine vibration decrement. Similar to the section impacts of input parameters on engine vibration, these results were the effect of increment in CNG addition and biodiesel blend ratio. The engine noise severity is given by equation (10).

$$\begin{aligned} \mathrm{dB[A]} = {} & 146.71 - 0.722X_1 - 0.0875X_2 \\ & - 0.06412X_3 + 0.03450{X_1}^2 \\ & + 0.001469{X_2}^2 + 0.000020{X_3}^2 \\ & + 0.00050X_1X_2 + 0.000017X_1X_3 \\ & + 0.000008X_2X_3. \end{aligned} \tag{10}$$

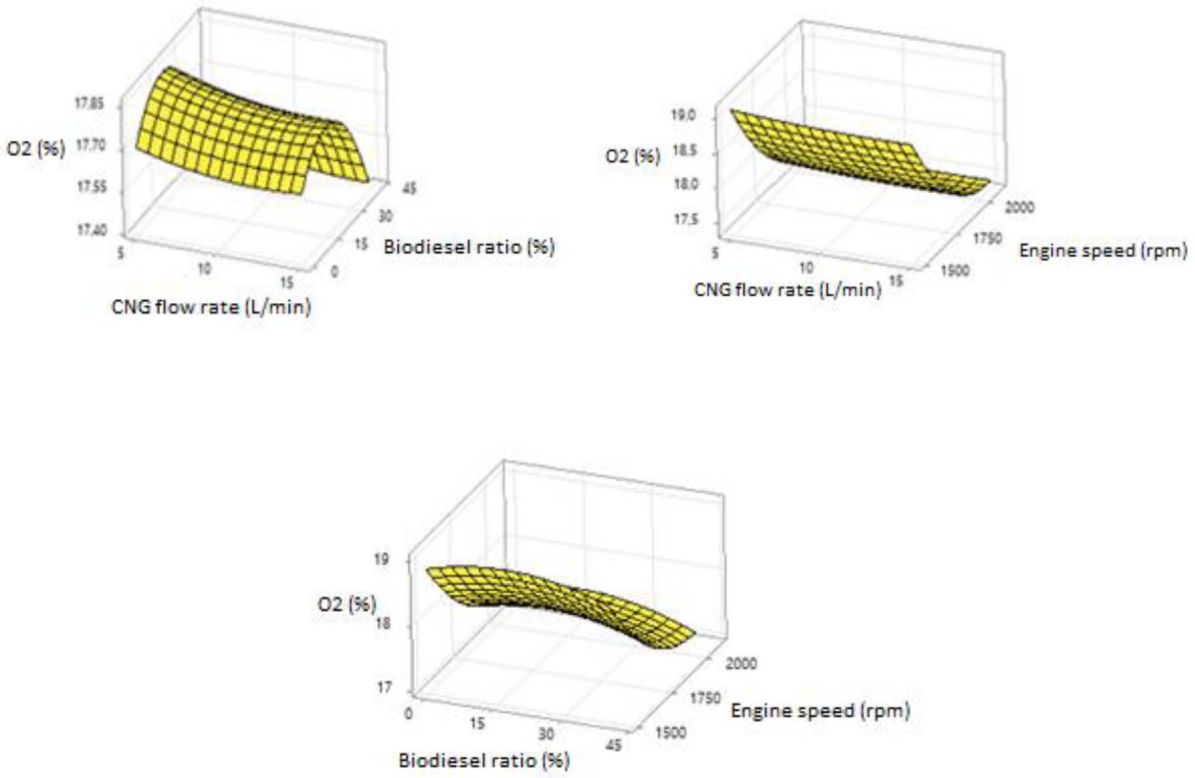

Fig. 6. Impacts of input parameters on O_2 emissions.

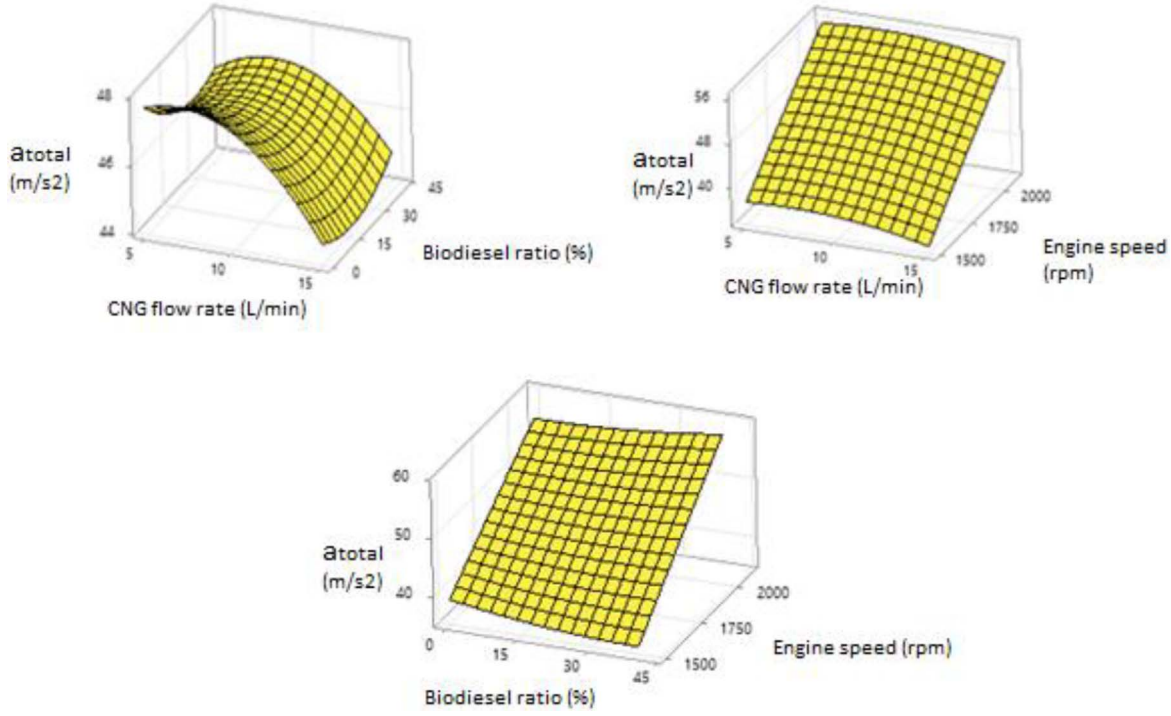

Fig. 7. Impacts of input parameters on engine vibration.

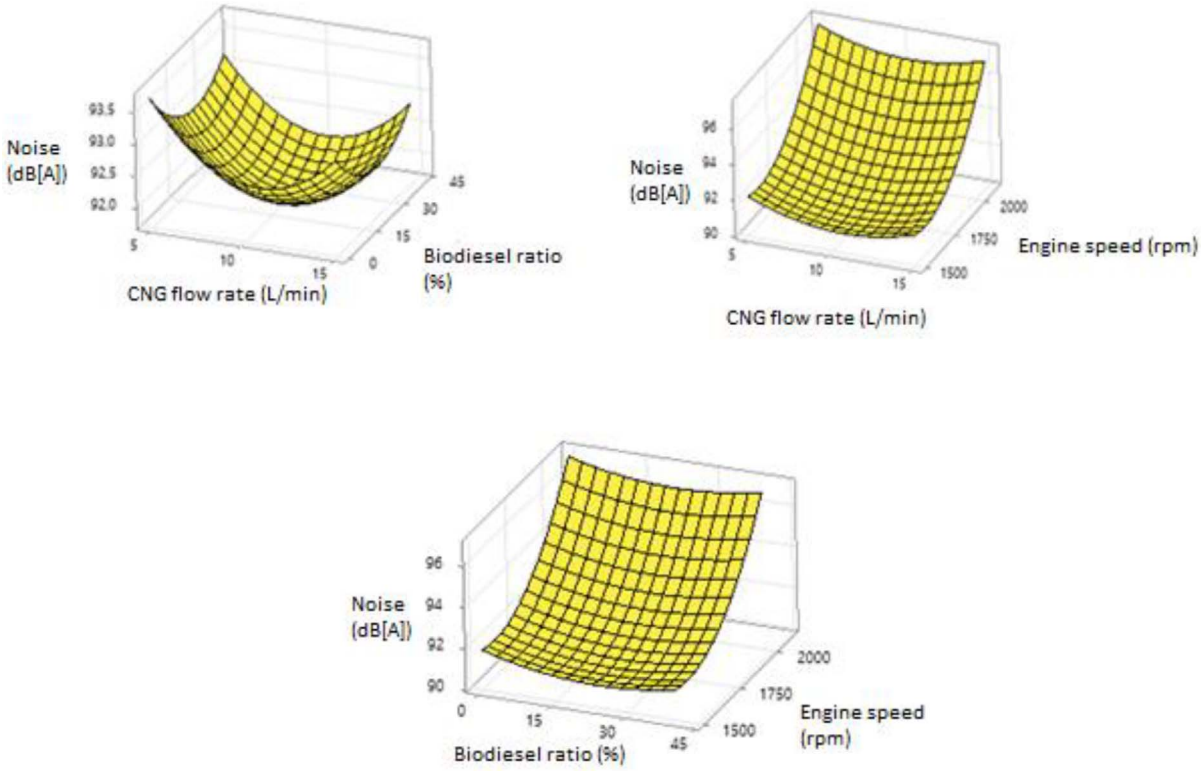

Fig. 8. Impacts of input parameters on noise.

Table 9. Optimisation of test setup and desirability of engine responses.

Response	Goal	Lower	Upper	Weight	Importance	Desirability
CNG addition (L/min)	In range	5	15	1	1	1
Biodiesel ratio (%)	In range	0	40	1	1	1
Engine speed (rpm)	In range	1500	2100	1	1	1
NO_x (ppm)	Minimum	64.00	153.00	1	1	0.66548
CO (ppm)	Minimum	312.00	765.00	1	1	0.72174
CO_2 (%)	Minimum	1.28	2.30	1	1	0.81409
O_2 (%)	Minimum	17.08	19.15	1	1	0.26804
Vibration (m/s^2)	Minimum	34.60	57.40	1	1	0.88730
Noise (dB[A])	Minimum	91.20	97.40	1	1	0.97670
Combined	–	–	–	–	–	0.6710

3.8 Optimisation and validation

Table 9 provides the optimisation criteria for dependent variables. Figure 9 demonstrates the obtained optimum input parameters and output values from canola biodiesel optimisation.

The optimum engine responses were found at 93.77 ppm, 438.05 ppm, 1.47%, 18.59%, 37.17 m/s^2 and 91.34 dB[A] for NO_x, CO, CO_2, O_2, and engine VN respectively. These values were for optimum input parameters at 9.24 L/min of CNG addition, 40% biodiesel blend ratio, and 1524.24 rpm of engine speed. Engine tests were carried out to validate the optimal solution and the results are shown in Table 10.

The engine test results were compared with RSM optimiser values. The errors were calculated using equation (11) [24].

$$\text{Error} = \frac{\text{Engine test result} - \text{Optimised result}}{\text{Engine test result}} * 100. \tag{11}$$

The errors for NO_x, CO, CO_2, O_2, and engine VN were 4.2%, 3.8%, 4.9%, 0.25%, 4.12%, and 0.17% respectively. From previous literature [19], all error values were within the acceptable limit.

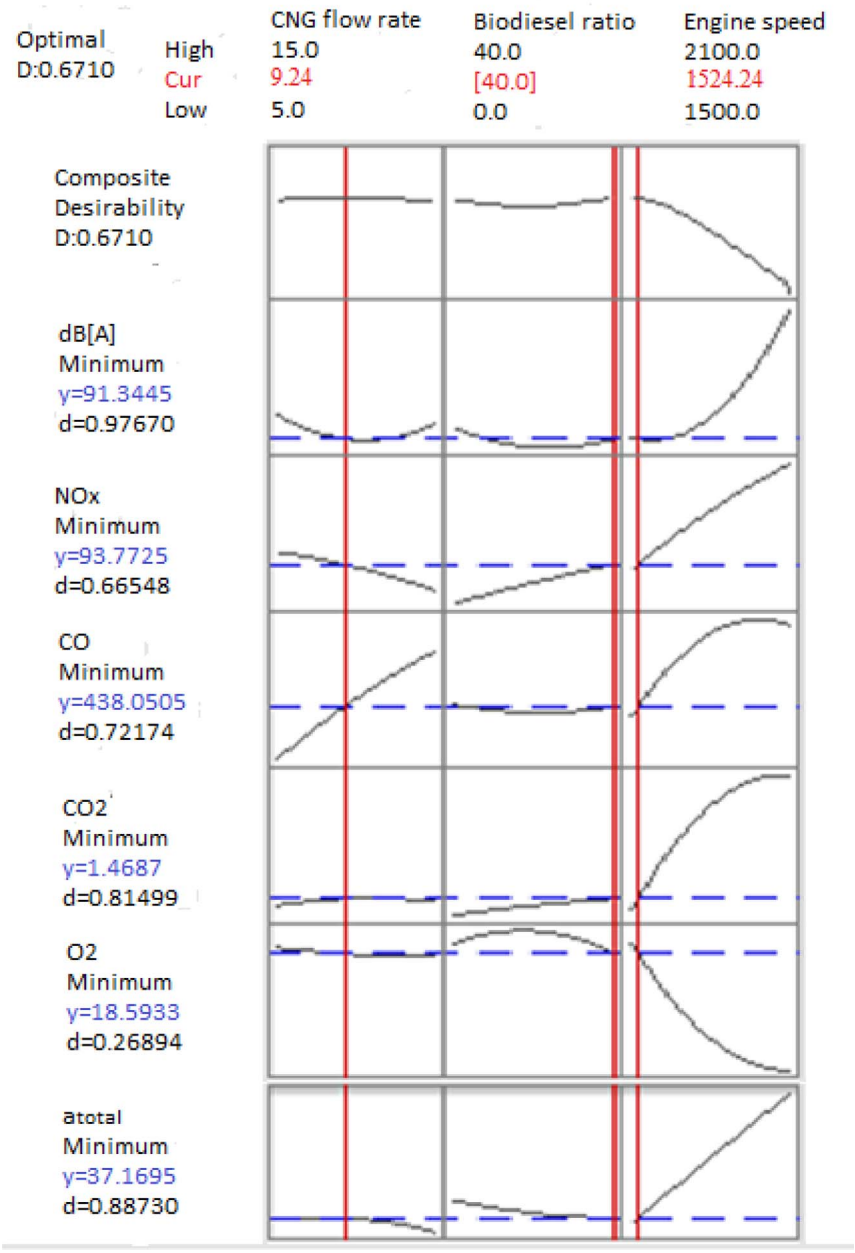

Fig. 9. Optimisation of NO_x, CO, CO_2, O_2 exhaust emissions and engine NV.

Table 10. Validation of engine test results.

CNG addition (L/min)	Biodiesel ratio (%)	Engine speed (rpm)	Value	NO_x (ppm)	CO (ppm)	CO_2 (%)	O_2 (%)	Vibration (m/s^2)	Noise (dB[A])
9.24	40	1524.24	Optimised result	93.77	438.05	1.47	18.59	37.17	91.34
			Engine test result	90	422	1.40	18.64	35.7	91.5
			Error %	4.2	3.8	4.9	0.25	4.12	0.17

4 Conclusions

The impacts of input parameters such as CNG addition, canola biodiesel blend ratio, and engine speed on the engine responses (exhaust emissions, and engine VN) were investigated during engine tests. The RSM model was successfully utilised to predict and optimise the measured engine responses. The results from the study can be summarised into four segments. 1) The highest approachable desirability was 0.6710 in the optimal operating parameters at 9.24 L/min CNG addition, 40% biodiesel ratio, and 1524.24 rpm engine speed. 2) The optimum engine responses of NO_x, CO, CO_2, O_2, and engine VN were obtained at 93.77 ppm, 438.05 ppm, 1.47%, 18.59%, 37.17 m/s^2, and 91.34 dB[A], respectively. 3) The coefficient determination of R^2 for NO_x, CO, CO_2, O_2, and engine VN were 99.11%, 99.22%, 99.41%, 99.70%, 98.65%, and 98.60% respectively. 4) The errors between the optimised result and the engine test result for NO_x, CO, CO_2, O_2, and engine VN were 4.2%, 3.8%, 4.9%, 0.25%, 4.12%, and 0.17% respectively. These errors were within the acceptable limit.

Conflicts of interest

No potential conflict of interest was reported by the authors.

References

1 Fangfang F., Alagumalai A., Mahian O. (2021) Sustainable biodiesel production from waste cooking oil: ANN modeling and environmental factor assessment, *Sustain. Energy Technol. Assess* **46**, 101265.

2 Qadeer M.U., Ayoub M., Komiyama M., Daulatzai M.U.K., Mukhtar A., Saqib S., Ullah S., Qyyum M.A., Asif S., Bokhari A. (2021) Review of biodiesel synthesis technologies, current trends, yield influencing factors and economical analysis of supercritical process, *J. Clean. Prod.* **309**, 127388.

3 Helmiyati H., Budiman Y., Abbas G.H., Dini F.W., Khalil M. (2021) Highly efficient synthesis of biodiesel catalyzed by a cellulose@ hematite-zirconia nanocomposite, *Heliyon* **7**, 3, e06622.

4 Silva G.S., Marques E.L.S., Dias J.C.T., Lobo I.P., Gross E., Brendel M., da Cruz R.S., Rezende R.P. (2012) Biodegradability of soy biodiesel in microcosm experiments using soil from the Atlantic Rain Forest, *Appl. Soil Ecol.* **55**, 27–35.

5 Çelebi K., Uludamar E., Tosun E., Yıldızhan Ş., Aydın K., Özcanlı M. (2017) Experimental and artificial neural network approach of noise and vibration characteristic of an unmodified diesel engine fuelled with conventional diesel, and biodiesel blends with natural gas addition, *Fuel* **197**, 159–173.

6 Shojae K., Mahdavian M., Khoshandam B., Karimi-Maleh H. (2021) Improving of CI engine performance using three different types of biodiesel, *Process Saf. Environ. Prot.* **149**, 977–993.

7 Felayati F.M., Semin, Cahyono B., Bakar R.A., Birouk M. (2021) Performance and emissions of natural gas/diesel dual-fuel engine at low load conditions: Effect of natural gas split injection strategy, *Fuel* **300**, 121012.

8 Shen Z., Wang X., Zhao H., Lin B., Shen Y., Yang J. (2021) Numerical investigation of natural gas-diesel dual-fuel engine with different piston geometries and radial clearances, *Energy* **220**, 119706.

9 Tosun E., Özcanlı M. (2021) Hydrogen enrichment effects on performance and emission characteristics of a diesel engine operated with diesel-soybean biodiesel blends with nanoparticle addition, *JESTECH* **24**, 3, 648–654.

10 Keskin A., Gürü M., Altiparmak D. (2007) Biodiesel production from tall oil with synthesized Mn and Ni based additives: Effects of the additives on fuel consumption and emissions, *Fuel* **86**, 7–8, 1139–1143.

11 Yang W.W., Tang X.Y., Ma X., Li J.C., Xu C., He Y.L. (2023) Rapid prediction, optimization and design of solar membrane reactor by data-driven surrogate model, *Energy* **285**, 129432.

12 Petcharat N., Wiangkham A., Pichitkul A., Tantrairatn S., Aengchuan P., Bureerat S., Banpap S., Khunthongplatprasert P., Ariyarit A. (2023) The multi-objective optimization of material properties of 3D print onyx/carbon fiber composites via surrogate model, *Mater. Today Commun.* **37**, 107362.

13 Aubeelack H., Segonds S., Bes C., Druot T., Brezillon J., Bérard A., Duffau M., Gallant G. (2023) Surrogate model development for optimized blended-wing-body aerodynamics, *J. Aircraft* **60**, 2, 437–448.

14 Das S., Kashyap D., Bora B.J., Kalita P., Kulkarni V. (2021) Thermo-economic optimization of a biogas-diesel dual fuel engine as remote power generating unit using response surface methodology, *TSEP* **24**, 100935.

15 Ye W., Wang X., Liu Y., Chen J. (2021) Analysis and prediction of the performance of free- piston Stirling engine using response surface methodology and artificial neural network, *Appl. Therm. Eng.* **188**, 116557.

16 Singh Y., Sharma A., Tiwari S., Singla A. (2019) Optimization of diesel engine performance and emission parameters employing cassia tora methyl esters-response surface methodology approach, *Energy* **168**, 909–918.

17 Adam I.K., Aziz A.A.R., Yusup S., Heikal M.R. (2016) Optimization of performance and emissions of a diesel engine fuelled with rubber seed- palm biodiesel blends using response surface method, *Asian J. Appl. Sci.* **4**, 2, 401–421.

18 Said Z., Le D.T.N., Sharma P., Dang V.H., Le H.S., Nguyen D.T., Bui T.A.E., Nguyen V.G. (2022) Optimization of combustion, performance, and emission characteristics of a dual-fuel diesel engine powered with microalgae-based biodiesel/diesel blends and oxyhydrogen, *Fuel* **326**, 124987.

19 Shirneshan A., Almassi M., Ghobadian B., Borghei A.M., Najafi G. (2016) Response surface methodology (RSM) based optimization of biodiesel-diesel blends and investigation of their effects on diesel engine operating conditions and emission characteristics, *Environ. Eng. Manag. J.* **15**, 12, 2771–2780.

20 Simsek S., Uslu S., Simsek H., Uslu G. (2021) Improving the combustion process by determining the optimum percentage of liquefied petroleum gas (LPG) via response surface methodology (RSM) in a spark ignition (SI) engine running on gasoline-LPG blends, *Fuel Process Technol.* **221**, 106947.

21 Singh T.S., Rajak U., Samuel O.D., Chaurasiya P.K., Natarajan K., Verma T.N., Nashine P. (2021) Optimization of performance and emission parameters of direct injection diesel engine fuelled with microalgae Spirulina (L.) –

Response surface methodology and full factorial method approach, *Fuel* **285**, 119103.

22 Krishnamoorthy V., Dhanasekaran R., Rana D., Saravanan S., Kumar B.R. (2018) A comparative assessment of ternary blends of three bio-alcohols with waste cooking oil and diesel for optimum emissions and performance in a CI engine using response surface methodology, Energy Convers. Manag. 156, September 2017, 337–357.

23 Subbaiah M.V., Reddy S.S.K., Prasad B.D. (2022) Optimization of performance and emission characteristics of common direct injection diesel engine using response surface methodology, *Mater. Today Proc.* **68**, 1294–1304.

24 Kumar A.N., Kishore P.S., Brahma Raju K., Ashok B., Vignesh R., Jeevanantham A.K., Nanthagopal K., Tamilvanan A. (2020) Decanol proportional effect prediction model as additive in palm biodiesel using ANN and RSM technique for diesel engine, *Energy* **213**, 119072.

25 Sharma A., Singh Y., Singh N.K., Singla A. (2019) Sustainability of jojoba biodiesel/diesel blends for DI diesel engine applications- taguchi and response surface methodology concept, *Ind. Crops. Prod.* **139**, 111587.

26 Patel P.D., Lakdawala A., Patel R.N. (2016) Box–Behnken response surface methodology for optimization of operational parameters of compression ignition engine fuelled with a blend of diesel, biodiesel and diethyl ether, *Biofuels* **7**, 2, 87–95.

27 Ramachander J., Gugulothu S.K., Sastry G.R.K., Panda J. K., Siva Surya M. (2021) Performance and emission predictions of a CRDI engine powered with diesel fuel: A combined study of injection parameters variation and Box–Behnken response surface methodology based optimization, *Fuel* **290**, 120069.

28 How H.G., Masjuki H.H., Kalam M.A., Teoh Y.H. (2018) Influence of injection timing and split injection strategies on performance, emissions, and combustion characteristics of diesel engine fueled with biodiesel blended fuels, *Fuel* **213**, 106e14.

29 Uslu S. (2020) Optimization of diesel engine operating parameters fueled with palm oil-diesel blend: Comparative evaluation between response surface methodology (RSM) and artificial neural network (ANN), *fuel* **276**, 117990.

30 Şimşek S., Uslu S. (2020) Investigation of the effects of biodiesel/2-ethylhexyl nitrate (EHN) fuel blends on diesel engine performance and emissions by response surface methodology (RSM), *Fuel* **275**, 118005.

31 Polat S. (2016) An experimental study on combustion, engine performance and exhaustemissions in a HCCI engine fuelled with diethyl ether–ethanol fuel blends, *Fuel Process Technol.* **143**, 140–150.

32 Paul A., Panua R.S., Debroy D., Bose P.K. (2014) Effect of compressed natural gas dual fuel operation with diesel and pongamia pinnata methyl ester (PPME) as pilot fuels on performance and emission characteristics of a CI (compression ignition) engine, *Energy* **68**, 495–509.

33 Pulkrabek W.W. (1997) *Engineering Fundamentals of the Internal Combustion Engine*, Pearson, New Jersey, USA, pp. 229–261.

34 Hoang A.T. (2021) Combustion behavior, performance and emission characteristics of diesel engine fuelled with biodiesel containing cerium oxide nanoparticles: A review, *Fuel Process Technol.* **218**, 106840.

35 Cheikh K., Sary A., Khaled L., Abdelkrim L., Mohand T. (2016) Experimental assessment of performance and emissions maps for biodiesel fueled compression ignition engine, *Appl. Energy* **161**, 320–329.

36 Yaşar A., Keskin A., Yıldızhan Ş., Uludamar E. (2019) Emission and vibration analysis of diesel engine fuelled diesel fuel containing metallic based nanoparticles, *Fuel* **239**, 1224–1230.

37 Yusaf T.F., Buttsworth D.R., Saleh K.H., Yousif B.F. (2010) CNG-diesel engine performance and exhaust emission analysis with the aid of artificial neural network, *Appl. Energy* **87**, 5, 1661–1669.

38 Hazar H., Tekdogan R., Sevinc H. (2021) Investigating the effects of oxygen enrichment with modified zeolites on the performance and emissions of a diesel engine through experimental and ANN approach, *Fuel* **303**, 121318.